Journal of
Composites Science

Article

Analysis of the Degradation During Melt Processing of PLA/Biosilicate® Composites

Eduardo H. Backes [1,*], Laís de N. Pires [1], Lidiane C. Costa [2], Fabio R. Passador [3] and Luiz A. Pessan [2]

[1] Graduate Program in Materials Science and Engineering, Federal University of São Carlos, Via Washington Luiz, Km 235, 13565-905 São Carlos, SP, Brazil; lais_pires77@hotmail.com
[2] Department of Materials Engineering, Federal University of São Carlos, Via Washington Luiz, Km 235, 13565-905 São Carlos, SP, Brazil; lidiane@ufscar.br (L.C.C.); pessan@ufscar.br (L.A.P.)
[3] Science and Technology Institute. Federal University of São Paulo, Talim St. 330, 12231-280 São José dos Campos, SP, Brazil; fabiopassador@gmail.com
* Correspondence: ehbackes@gmail.com

Received: 9 April 2019; Accepted: 13 May 2019; Published: 16 May 2019

Abstract: Poly (lactic acid) (PLA)/bioactive composites are emerging as new biomaterials since it is possible to combine stiffness, mechanical resistance, and bioactive character of the bioglasses with conformability and bioabsorption of the PLA. In this study, PLA/Biosilicate® composites were prepared using a melt-processing route. The processability and properties were evaluated aiming to produce composites with bioactive properties. Two different PLA (PLA 2003D and PLA 4043D) were tested with the addition of 1 wt. % of Biosilicate®. Both materials presented a huge reduction in melt viscosity after internal mixer processing. The degradation effects of the addition of Biosilicate® in the PLAs matrices were evaluated using zeta potential tests that showed a very high liberation of ions, which catalyzes PLA thermo-oxidative reactions. To understand the extension of degradation effects during the processing, the composites were characterized using thermogravimetric analysis (TGA), differential scanning calorimetry (DSC), gel permeation chromatography (GPC), and rheological tests. GPC results showed that PLA with the lowest residual acid content (RAC), PLA 2003D, presented higher thermal stability, higher molecular weight, and viscosity baseline compared to PLA 4043D. The composites showed a significant decrease in molecular weight for both PLA with the addition of Biosilicate®. TGA results showed that Biosilicate® might have reduced the activation energy to initiate thermodegradation reactions in PLAs and it occasioned a reduction in the T_{onset} by almost 40 °C. The DSC results showed that severe matrix degradation and the presence of bioglass did not significantly affect glass transition temperature (T_g), melting temperature (T_m) and crystallinity of PLAs, but it influenced cold crystallization peak (T_{cc}). In this way, the type of PLA used influences the processability of this material, which can make the production of filaments of this material for 3D printing unfeasible.

Keywords: poly (lactic acid); Biosilicate®; melt compounding; biomaterial; degradation

---

1. Introduction

Poly (lactic acid) (PLA) is a polyester and presents good mechanical properties and biocompatibility, and it is bioabsorbable [1]. Due to these characteristics, the PLA is being widely used in medical applications such as intradermal sutures, fracture recovery devices and tissue regeneration (TR) [2,3]. However, PLA does not present osteoinduction behavior when implanted, and one way of conferring this property to it is through the addition of bioactive fillers [4,5]. The bioglass developed by Hench (45S5) is the "gold standard" for bone implants; however, other highly bioactive materials have been discovered, as Biosilicate®. Biosilicate® has been used in the dental area to treat dentin hypersensitivity, due to its osteoinductive and osteoconductive properties it aids bone healing and growth [6]. It is interesting to observe that Biosilicate® also has the potential to be applied in antibacterial coatings due to its antimicrobial properties that inhibit bacterial activity [7]. It is interesting to point out that this intrinsic property of Biosilicate® resulted in a considerable reduction of the anaerobic bacteria after 10 min contact tests [7]. Granito et al. [8,9] implanted 45S5 and Biosilicate® glasses in rat tibial defects and it was observed that Biosilicate® was more tenacious and more bioactive when compared to the gold standard of the bioglasses (45S5). Biosilicate® has been widely researched (over 30 scientific papers and 28 theses) and it was demonstrated that this material is highly bioactive and can be used for bone tissue regeneration [9]. PLA/bioglass composites represent a promising class of materials which can be applied in the tissue regeneration because these composites combine the flexibility, conformability, and bioabsorption capacity of PLA and at the same time combine the stiffness, mechanical resistance, and bioactivity of the bioglasses [8]. The current techniques used for the preparation of PLA/bioglass composites are based mainly on the use of a solvent such as solvent casting-particulate leaching [10,11] and phase inversion [5,12]. Blaker et al. [13] produced PLA scaffolds with different contents of bioglass by the phase inversion method and then evaluated the formation of hydroxyapatite on the surface of the scaffolds after different immersion times in simulated body fluid (SBF). The SBF test evaluated the in vitro bioactivity of biomaterials and it was observed that in the PLA/bioglass composite (95/5 m/m) the formation of hydroxyapatite occurred after only 3 days of immersion. These results are a strong evidence of the bioactivity potential of bioglasses; however further bioactive properties were assessed with cell lines cultures. The authors performed infiltration of osteoblasts into these scaffolds and noted that the cells were able to migrate through the pores of the scaffolds and colonize even deeper regions, indicating that these materials have a biochemical structure and composition capable of supporting the bonds of osteoblasts [13].

The main disadvantage of phase inversion and solvent casting-particulate leaching methods is the use of solvents which, in most cases, are toxic and can remain in the scaffold produced. In the area of preparation of scaffolds, other methods are being applied, such as 3D printing. However, it is necessary to modify the filament to produce scaffolds for bone tissue regeneration using this technique. Cunha et al. [14] produced 3D scaffolds of PCL/Biosilicate® and the observed improvement in the mechanical properties and the addition of Biosilicate® provided a good environment for cell attachment and proliferation [14]. It is worth noticing that the printed scaffold used a specific printing setup where the two separated materials were feed in powder form which may lead to some drawbacks as poor filler dispersion. In this work, a different route is proposed to obtain PLA/Biosilicate® composites. The aim of this study was the development of melt-processed PLA/Biosilicate® composites using an internal melt mixer. Two different PLA's were used for composites production and were analyzed through thermogravimetric analysis (TGA), rheological behavior, and molar mass characterization. The effect of Biosilicate® addition on PLA matrices by this type of processing is promising for the preparation of filaments to produce 3D scaffolds for bone tissue regeneration.

2. Materials and Methods

2.1. Materials

PLA matrix: Two different PLA matrices were used in this study, PLA 2003D and PLA 4043D; both were provided my Natureworks® (Minnetonka, MN, USA). PLA 2003D it is a grade specific for extrusion, D-isomer of 3.5 wt. %, and has molecular weight around 120.000 g/mol whereas PLA 4043D is specific for films, D-isomer from 4.5–5 wt. % and has molecular weight around 110.000 g/mol. The Biosilicate® used is a quaternary system of $23.75Na_2O$–$23.75CaO$–$48.5SiO_2$–$4P_2O_5$ (wt. %), average particle size (d_{50}) of approximately 5 μm and was kindly provided by Vitreous Materials Laboratory (LaMaV)/Federal University of São Carlos (São Carlos, Brazil) [6–9].

2.2. Methods

2.2.1. Preparation of Poly (lactic acid) (PLA)/Biosilicate® Composites

Internal Mixer (Torque Rheometer, Thermo Fisher Scientific, Karlsruhe, Germany) Processing: The different PLAs matrices with Biosilicate® (1 wt. %) were processed using an internal mixer (torque rheometer), Haake Rheomix 600p. The mixing time was 5 min, rotation of 60 rpm and 185 °C. To improve the mixing of the PLA with Biosilicate®, the PLAs were cryogenically milled. The PLAs were dried under vacuum for 4 h at 70 °C and Biosilicate® at 120 °C for 24 h in a forced air convection oven.

2.2.2. Characterization of Biosilicate®

Biosilicate® was characterized by zeta potential. The test was performed with the purpose of analyzing the surface characteristics of Biosilicate® in aqueous solution, i.e., the electrical conductivity and pH variation over time. The assay was performed on a zeta potential analyzer, model ESA 9800. For the preparation of the solutions, the dispersing agent (Darvan) was used at 1 wt. % relative to the mass of Biosilicate®, with a concentration of Biosilicate® at 25 wt. % of the water mass.

2.2.3. PLAs Matrices and PLA/Biosilicate® Composites Characterization

Rheological characterization: The rheological behavior of the different PLA's and composites was evaluated, using a controlled stress rheometer AR G2 (TA Instruments) with parallel plate test geometry (25 mm) and 1 mm gap distance. The tests were conducted in an inert nitrogen atmosphere at 185 °C and the variation of the viscosity versus shear rate was analyzed.

Gel permeation chromatography (GPC): GPC was performed on the neat PLAs (pellets and after processing in torque rheometer) and in the composites. The samples were solubilized in Tetrahydrofuran (Sigma-Aldrich, Steinheim, Germany) at 50 °C and analyzed using a GPC Viscotek HT Module 350a at pump flow of 1 mL/min. The GPC calibration curves were obtained from polystyrene (PS) standards.

PLA residual acid content (RAC): The RAC of the PLAs was determined by the titration of the PLA chain end. Briefly, 1.0 g of sample was solubilized in chloroform (1/100 wt./wt.) and titrated with KOH (0.05 M). Thereafter, an excess of KOH was added, approximately 0.200 mL. Reverse titration of the excess was performed using a solution of HCl (0.05M). The determination of the RAC of PLAs was performed in triplicate from 3 different PLA pellets.

The PLA acid content was determined using Equation (1).

$$\text{Acid Content (\%)} = ((V_e \times \mathrm{C_{KOH}} \times \mathrm{M_{ga}})/(\mathrm{m_a})) \times 100 \tag{1}$$

where V_e is the volume of added equivalent KOH (VKOH + Vexcess − VHCl), $\mathrm{C_{KOH}}$ is the molar concentration of KOH, $\mathrm{M_{ga}}$ is the molar mass of the acid group of PLA (45 g mol^{-1}) and $\mathrm{m_a}$ is the mass of the sample.

Thermogravimetric analysis (TGA): The thermal stability of PLAs and the composites was evaluated using TGA analysis. The samples were heated from room temperature to 750 °C at a heating rate of 20 °C/min under nitrogen atmosphere (Platinum crucible) in a TGAQ50 (TA Instruments, New Castle, DE, USA).

Differential Scanning Calorimetry (DSC): The DSC technique was used to evaluate the thermal transitions and crystallinity of PLA and its variation with the addition of Biosilicate®. The analysis was conducted in a TA Instruments equipment, model QS100, using nitrogen as purge gas in a continuous flow of 50 mL min^{-1}. Samples were initially heated from 0 °C to 200 °C at a heating rate of 10 °C/min. The $\boldsymbol{T_g}$ value of the samples was obtained at the second heating cycle. The crystallinity was determined from the area of the DSC endotherm using 93.0 J/g as the heat of fusion of 100% crystalline PLA [1]. The apparent degree of crystallinity (X_c) can be determined using Equation (1):

$$X_c(\%) = \frac{(\Delta H_m - \Delta H_{cc})}{\varphi_i \Delta H_m^{\circ}} \times 100$$

where ΔH_m° is the absolute value of the heat of fusion measured for the PLA, ΔH_{cc} is the absolute value of crystallization measured at the exothermic peak of cold crystallization (only for the PLA phase), φ_{i} is the weight fraction of PLA in the composites, and ΔH_m° is the enthalpy of fusion of 100% crystalline PLA.

3. Results and Discussion

In this study, PLA and PLA/Biosilicate® composites were processed using an internal melt mixer. Two different PLA's were investigated, and Figure 1 presents the curves of torque versus time obtained by torque rheometry for the both PLAs (PLA 4043D and PLA 2003D) and PLA/Biosilicate® composites with the addition of 1wt% of Biosilicate®. The torque peak corresponds to the addition of the compounds. Comparing the results of the different neat PLAs (Figure 1a,b), it is observed that the maximum torque of PLA 4043D is 73 N m and for the PLA 2003D is 65 N m. The addition of Biosilicate® changes the maximum torque values for both composites, being more evident for the composite with PLA 4043D. In Figure 1a it is possible to observe that PLA 4043D presents constant torque (3.9 N m) from 1 to 5 min of mixing and the addition of only 1 wt. % of Biosilicate® resulted in a continuous decrease in torque obtaining a significantly lower value (1.1 N m) compared to neat PLA 4043D. In Figure 1b is observed that PLA 2003D shows a similar behavior as PLA 4043D, i.e., the torque is constant from 1 to 5 min. However, for this PLA 2003D, the torque at 5 min is higher than for PLA 4043D (3.1 N m for PLA 2003D and 1.1 N m for PLA 4043D). The addition of Biosilicate® in PLA 2003D also caused a decrease in the torque during the processing of the composite. The continuous decrease of torque during processing may be associated with the degradation process with the breaking of the polymer chains. The literature shows that the main reaction of the thermo-oxidative degradation mechanism of PLA (neat) is non-radical with intramolecular transesterification. The reactions involved during the thermal degradation of PLA are non-radical scission, backbiting ester interchange, cis-elimination and they are dependent of the hydroxyl groups at the end of PLA chain [15]. As these reactions proceed, several transitory residues are formed as lactide molecules, oligomeric ring, acetaldehyde with a double bond, volatiles and quite a few of these components have low molecular mass [16]. These reactions occur only at temperature above 270 °C [15,16]. However, thermo-oxidative degradation reactions can occur at temperatures below 270 °C due to the synergistic effect of oxygen and shear [16]. For both cases, Biosilicate® might have catalyzed degradation reactions as it can be noticed in Figure 2 that presents the visual appearance of both PLA after been processed in internal mixer. The neat PLAs did not present color change however, after the processing the sample with addition of Biosilicate® showed significant changes in the color from transparent yellowish to brown. This fact may be a strong evidence of polymer degradation and corroborates with the results of torque rheometry.

Aiming to understand the effect of the degradation during melt processing of the composites, the zeta potential test was performed for Biosilicate®. The zeta potential characterization not only provides information about the material's electrical conductivity but also how the pH of the solution changes with the time. The result is showed in Figure 3 and it is noticed a rapid increase in the electrical conductivity from 1 to 5 min, from 40 to 100 µs/cm, i.e., the material presents a huge release of ions in contact with aqueous solution. The dissolution of calcium and sodium in Biosilicate® contributes to the fast increase of the electrical conductivity and pH of the solution, and the rapid dissolution of calcium, which is one of the constituents of bone, might be responsible for Biosilicate® highly bioactivity [6–9]. Blaker et al. [17] have observed premature degradation of the PLA by addition of the 45S5 during thermal processing and attributed the early degradation of the PLA to the release of counterions of the

45S5 that catalyze thermal degradation reactions, as observed for Biosilicate®. Although zeta potential test is performed in aqueous solution, it is possible that Biosilicate® components might react with PLA matrix during mixing in molten state and thus the zeta potential provides useful information about Biosilicate® high bioactivity which is associated with the capacity of rapid dissolution of some counterions, such as calcium.

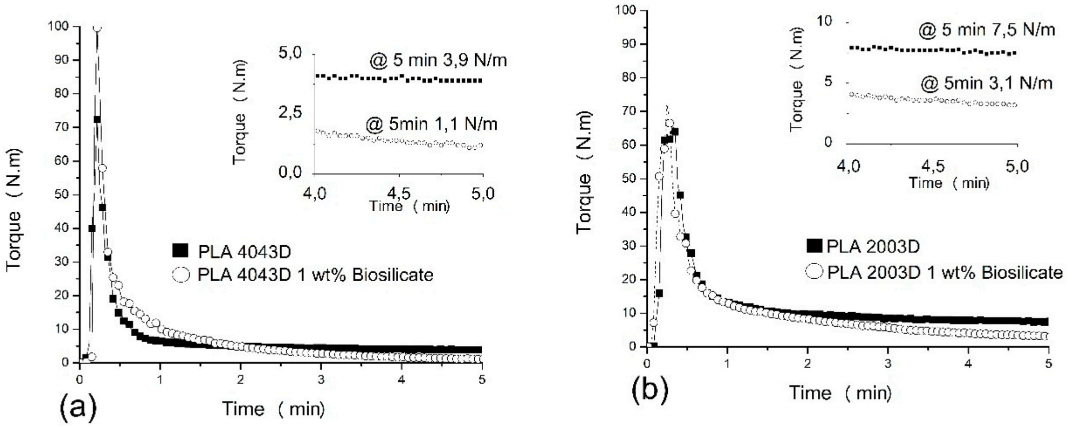

Figure 1. Torque versus time for Poly (lactic acid) (PLA) 4043D (**a**) and PLA 2003D (**b**) with and without Biosilicate®.

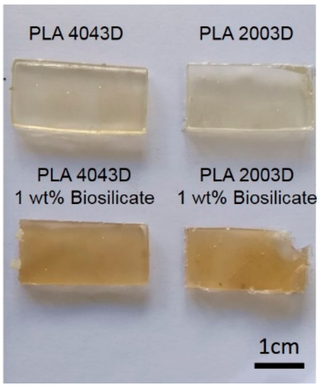

Figure 2. Samples obtained after processing in an internal mixer.

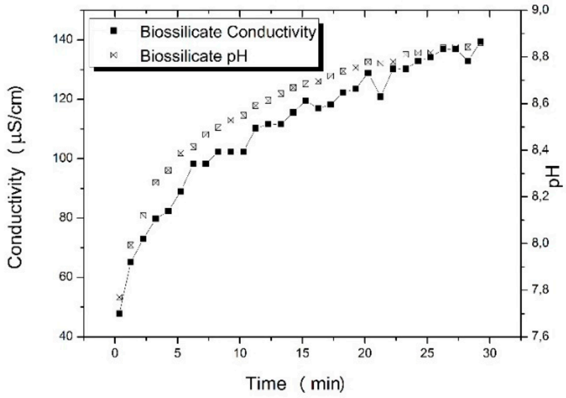

Figure 3. Zeta potential and conductivity of Biosilicate®.

Fan et al. [18,19] prepared PLA calcium ion end capped (PLA-Ca) by treating the PLA with CaH_2 and analyzed the thermodegradation of this material under pyrolysis. According to Fan et al., the calcium (Ca) act as a counterion accelerating nucleophilic substitution reactions (SN2) and leading to the racemization of PLA, i.e., the formation of meso-lactide. Another mechanism proposed by

Fan et al. [19] during pyrolysis of PLA-Ca is the random transfer between PLA chains. The reactions proposed are presented in Figure 4. Thus, it can be concluded that similar effects can occur with the PLA/Biosilicate® composites produced by torque rheometry.

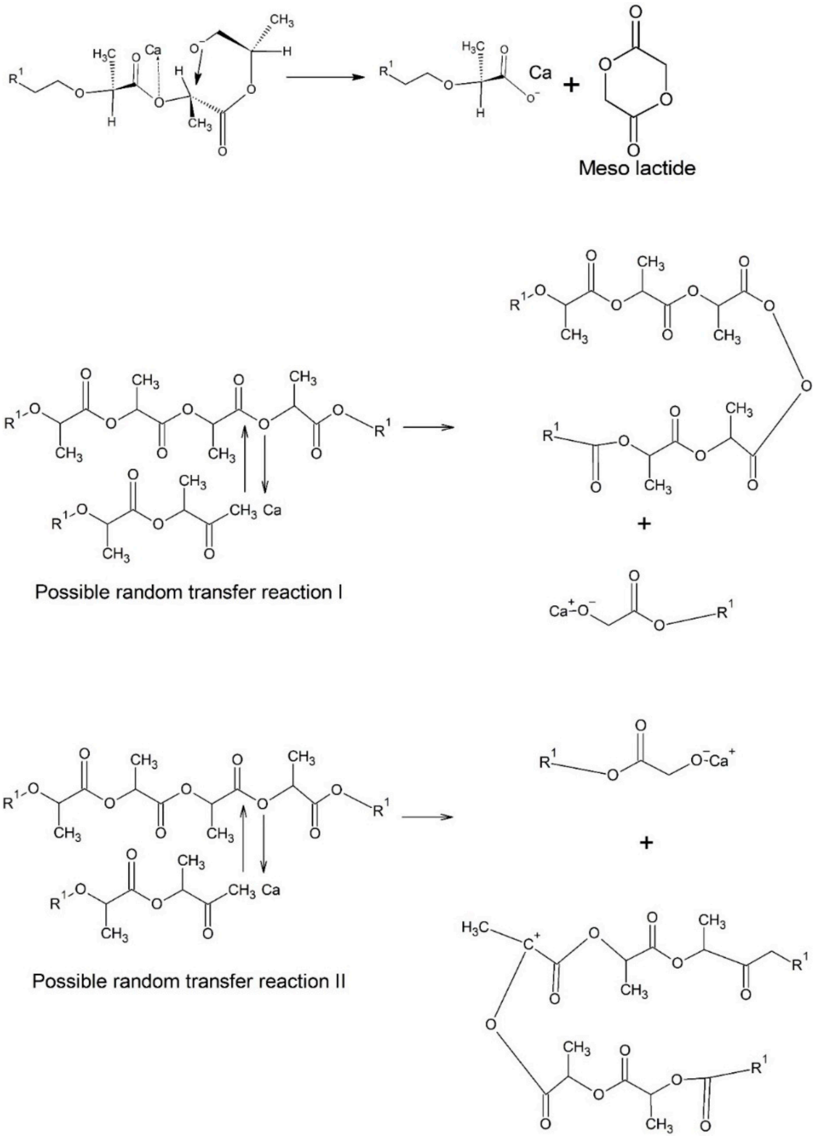

Figure 4. Meso-lactide formation by the SN2 reaction on asymmetrical methyne carbon and possible random transfer reactions in the initial period of PLLA-Ca pyrlosys. Adapted from [19].

To understand the effect of the degradation behavior during melt processing, the rheological behavior of the neat PLAs and the composites were evaluated. Figure 5 presents the curves of viscosity versus shear strain for the different PLAs and the composites of PLAs with 1 wt. % of Biosilicate®. The two PLAs used in this work have similar rheological behavior; however, PLA 2003D possess higher viscosity compared to PLA 4043D. The presence of Biosilicate® reduced the viscosity of both PLAs remarkably, although the viscosity variation presented by both composites remained equivalent when compared to the pure polymers. In addition, a change in the rheological behavior of the composites with the addition of Biosilicate® is noticed. Both PLAs present a Newtonian behavior (0.01 to 10 s^{-1}), i.e., the viscosity remained constant with increasing shear rate. The PLA/Biosilicate® composites exhibited shear thinning (pseudoplastic) behavior even at low shear rates and higher viscosity values than PLA in very low shear rates (up to 0.05 s^{-1}). These rheological results indicate that the addition of

Biosilicate® could have strongly affected the melt processing of the composites and contribute to the degradation of the PLA matrix.

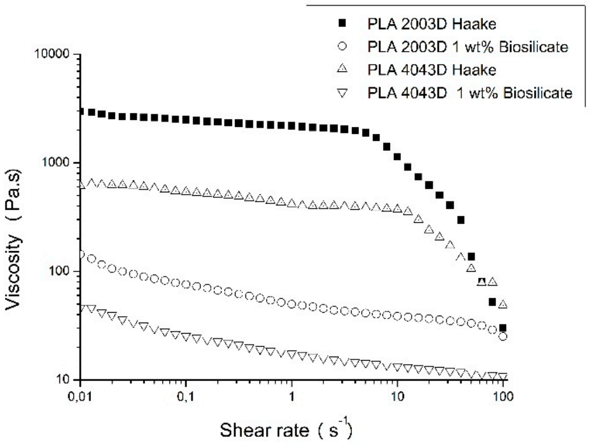

Figure 5. Viscosity versus shear rate for PLA 4043D and PLA 2003D.

Figure 6 presents the GPC curves of PLA 4043D (a) and PLA 2003D (b), pellets (as received), after torque rheometer (Haake) processing with and without Biosilicate® (Table 1) The results show that the PLA 2003D (as received) has a higher number average molar weight (Mn) than PLA 4043D. This result was expected since the PLA 2003D shows higher viscosity baseline when compared to PLA 4043D in the rheological analysis. It is interesting to note, however, that the PLA 2003D presented a reduction of 13% in the Mn and the weight average molecular weight (Mw) was the same after processing by torque rheometer when compared to their pellets (as received). On the other hand, the PLA 4043D presented a reduction of 30% in the Mn and 24% the Mw after processing when compared to its pellets.

To investigate the different behavior of the PLAs their RAC values were determined. The RAC in the PLAs comes from the different functional groups of PLA chain, which might be hydroxyl or carbonyl groups. The RAC in the PLA directly affects its stability and can make the material more susceptible to degradation during shearing process. This is because acidic conditions are known for catalyzing PLA hydrolysis reactions [15,16], i.e., the acid group presence in the system during the processing could enhance the degradation processes of the polymer, reducing its molar mass and viscosity. The RAC of the PLAs was determined by titration and a slight difference between them was observed. The PLA 2003D presented acid content of 0.20 ± 0.02% while PLA 4043D 0.30 ± 0.01% [20,21]. The difference in RAC for both PLAs corroborates their performance (viscosity and molar mass) after processing. However, PLA 2003D was less sensitive to degradation since it maintained higher M_n and M_w compared to PLA 4043D. On the contrary, the addition of 1 wt. % of Biosilicate® led to the pronounced shift of the GPC curves to the left side when the Biosilicate® was added. It was the result of a similar decrease in Mn and Mw for both PLAs, ranging from 50 to 60% of decrease molar mass. As already mentioned, the PLA degradation reactions involved during the processing carried out are thermal degradation under shear, hydrolytic degradation (catalyzed by acid groups—OH and COOH) and thermodegradation in the presence of the calcium ion. Therefore, the results suggest that there may be a predominance of thermodegradation in the presence of the calcium ion during the mixture in the molten state of the PLA with the Biosilicate®. This can be explained by equivalent reductions of the molar mass independent of the RAC.

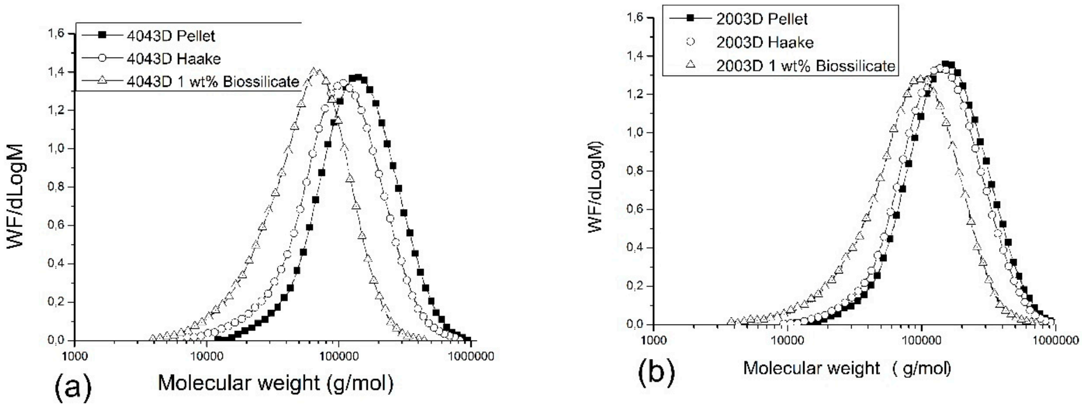

Figure 6. Gel permeation chromatography (GPC) curves of PLA 4043D (**a**) and PLA 2003D (**b**), with and without 1 wt. % Biosilicate®.

Table 1. Molar mass of the Poly (lactic acid) (PLAs) and PLAs with and without the addition of 1 wt. % of Biosilicate®.

Sample	PLA 4043D M_n/M_w (g/mol)	PLA 2003D M_n/M_w (g/mol)
Pellet (as received)	106000/168000	118600/168000
Haake (after processing)	74000/128000	103000/168000
1 wt. % Biosilicate®	43000/72000	59000/73000

The influence of PLA degradation was analyzed through thermal stability using TGA, while their thermal behavior before decomposition was registered in DSC. Figure 7 and Table 2 presents TGA results for the PLAs with and without 1 wt. % of Biosilicate®. The TGA curve (Figure 7a) for the two PLAs are similar and the T_{onset} presented for PLA 2003D and PLA 4043D is almost equal; however, Biosilicate® led in both cases to a strong decrease in the thermal stability of the composites, i.e., a reduction of almost 40 °C in the T_{onset} and approximately 30 °C in the Derivative weight loss (DWL) at Figure 7b demonstrating that the PLA underwent different pathways of thermodegradation [15,16]. Similar behavior was observed by Fan et al. [19], where the PLA-Ca, modified with calcium salts, presented a decrease in its thermal stability. The authors quantified the activation energy to initiate thermodegradation reactions and for PLA-Ca it was reduced for the half compared to the same PLA that underwent a process of purification [19]. It was also noticed that for the samples with the addition of the Biosilicate® the residue was higher than for the PLAs. It is attributed to the amount of Biosilicate® that under TGA test conditions are not decomposed. Another possible explanation for this increase in the residue is that Biosilicate® when present in the composites might lead to the formation of other degradation residues which are not decomposed in the temperature analyzed. Biosilicate® has in its composition high content of calcium and might underwent some of the reaction as shown in Figure 4, which directly influences in its thermal stability.

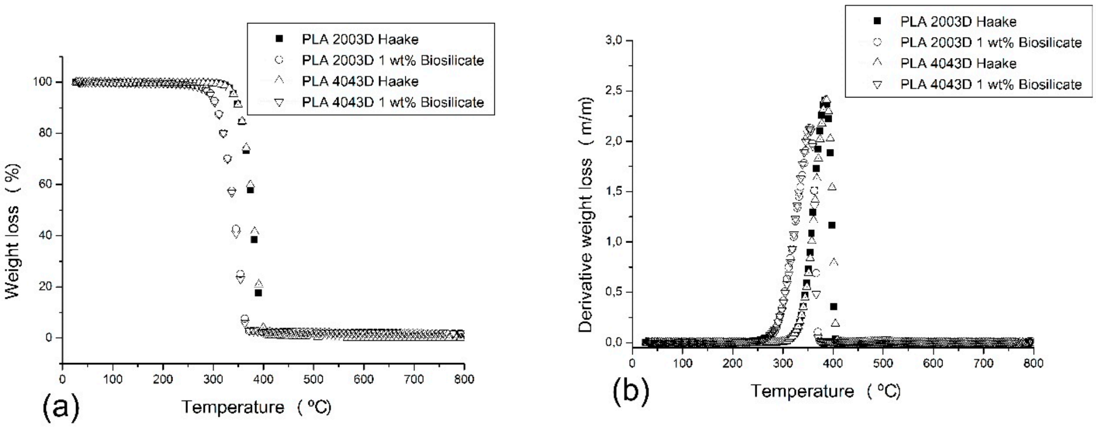

Figure 7. Thermogravimetric analysis (TGA) curves of PLA 2003D Haake, PLA 2003D 1 wt. % Biosilicate®, PLA 4043D Haake, and PLA 4043D 1 wt. % Biosilicate®. (**a**) Weight loss versus temperature, (**b**) Derivative weight loss versus temperature.

Table 2. Thermogravimetric analysis (TGA) results for the PLAs with and without 1 wt. % of Biosilicate®.

Sample	T_{onset} (°C)	DWL (°C)	The Residue (%)
PLA 4043D Haake	358	385	0.07
PLA 4043D 1 wt. % Biosilicate®	318	353	1.83
PLA 2003D Haake	356	384	0.10
PLA 2003D 1 wt. % Biosilicate®	319	353	1.80

Figure 8 shows DSC curves for the PLAs with and without 1 wt. % of Biosilicate® and the parameters calculated from those are presents in Table 3. The results of the second heating of all samples show that PLA was kept almost constant, approximately 60 °C, independent of the polymer molar mass and presence of Biosilicate®. However, when we analyzed the cold crystallization peak (T_{cc}), a shift towards higher temperatures, due to the increase of molecular mass (neat polymers) and the presence of bioglass (for both PLAs), is observed. This means that for the same heating condition, the crystallization of PLA occurs earlier in systems with greater flexibility and mobility of the chains because the molecules are shorter and allow the reorganization of amorphous domains [15]. PLA can crystallize into three polymorphic forms (α, β and γ) depending on process conditions. The α structure is more stable than the β structure and can be produced from the molten state [22]. The literature also reports the presence of an α crystalline phase that has a looser and disorderly structure, named α'. The crystallization of PLA in the temperature range from 100 to 120 °C can originate crystals α and α' at the same time [23]. In the PLA 4043D and PLA 4043D with addition of Biosilicate® it was observed one shoulder at the peak fusion of PLA and his evidence can indicate the contribution of both forms α and α'. The α' form, as mentioned earlier, has a disorderly structure and is fused at lower temperatures (T_{m1}) and then recrystallize in the form α, which is subsequently fused in higher temperatures (T_{m2}) [24]. Finally, the molar mass was reduced with the addition of Biosilicate® and it influenced the crystallinity percentage of the materials studied. During the cooling of the composite could occur crystallization the formation of more crystalline nuclei (due to the presence of bioglass particles), which would act as heterogeneous nuclei. This would facilitate the crystallization of the material [25]. The presence of bioglass could increase the crystallization rate of the PLA, and this would be demonstrated by a higher percentage of crystallization of the composite PLA, for a given cooling rate. For both PLA it was noticed a slight improvement in the crystallinity of the composites with addition of Biosilicate®; however, the results showed very low percentages of crystallinity for the studied materials, characterizing almost amorphous materials.

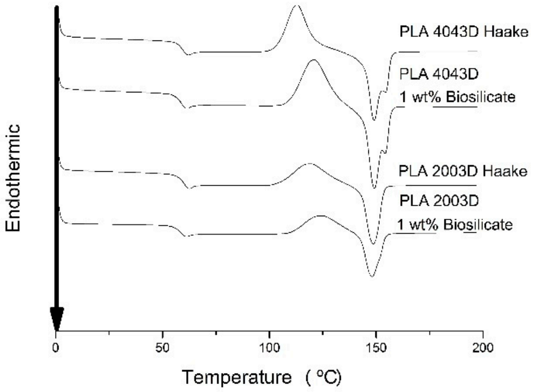

Figure 8. Heat flow rate versus temperature of PLA 4043D Haake, PLA 4043D 1 wt. % Biosilicate®; PLA 2003D Haake and PLA 2003D 1 wt. % Biosilicate® during second heating. Curves were displaced vertically for clarity.

Table 3. Thermal and Crystalline Properties of the PLAs with and without 1 wt. % of Biosilicate®.

Sample	T_g (°C)	T_{cc} (°C)	ΔH_{cc} (J/g)	T_{m1}/T_{m2} (°C)	ΔH_m (J/g)	X_c(%)
PLA 4043D Haake	60.9	113	25.50	149/154	25.6	0.07
PLA 4043D 1 wt. % Biosilicate®	59.3	121	30.40	149/154	30.6	0.23
PLA 2003D Haake	60.3	119	18.90	149/-	19.1	0.22
PLA 2003D 1 wt. % Biosilicate®	59.0	125	15.40	148/-	16.5	1.15

4. Conclusions

PLAs/Biosilicate® composites were prepared using a new route of processing by internal mixer rheometer aiming to obtain a new biomaterial for bone tissue regeneration. The high bioactivity of Biosilicate®, as demonstrated by zeta potential, lead to severe degradation of the two PLAs tested during the melt processing. PLA 2003D presents lower RAC and therefore presented higher thermal-oxidative resistance, which leads to higher viscosity baseline, M_n and M_w when compared to PLA 4043D. TGA results showed that Biosilicate® might have reduced the activation energy to initiate thermodegradation reactions in PLAs and it occasioned a reduction in the T_{onset} by almost 40 °C. DSC showed that only T_{cc} was influenced by the polymeric chains mobility and the presence of Biosilicate®. The addition of Biosilicate® might also act as nucleating crystallization sites in the composites; however, they presented low percentages of crystallinity, remaining amorphous. Thus, the melt processing of PLA/Biosilicate® composites is quite complicated, since Biosilicate® accelerates the PLA degradation process, requiring the addition of processing agents to prevent premature degradation of PLA during processing. This material has great potential to produce filaments for the 3D printing of scaffolds for bone tissue regeneration.

Author Contributions: Conceptualization, E.H.B., L.C.C., F.R.P. and L.A.P.; methodology, E.H.B.; software, E.H.B.; validation, E.H.B., L.C.C., F.R.P. and L.A.P.; formal analysis E.B., L.N.P., L.C.C., F.R.P. and L.A.P.; investigation, E.H.B., L.d.N.P.; resources, E.H.B., L.A.P.; data curation, E.H.B.; writing—original draft preparation, E.B., L.d.N.P.; writing—review and editing, L.C.C., F.R.P. and L.A.P.; visualization, E.B.; supervision, L.C.C., F.R.P. and L.A.P.; project administration, L.A.P.; funding acquisition E.H.B., L.C.C., F.R.P. and L.A.P.

Funding: This research was funded by Fundação de Amparo à Pesquisa do Estado de São Paulo (FAPESP) (grant number 2016/19978-9 and 2017/09609-9). This study was financed in part by the Coordenação de Aperfeiçoamento de Pessoal de Nível Superior (CAPES) – Brasil, Finance Code 001.

Acknowledgments: The authors would like to thanks to Marina Trevelin, Edgar Zanotto and Vitreous Materials Laboratory (LaMaV) for donating Biosilicate®.

Conflicts of Interest: The authors declare no conflict of interest.

References

1. Raquez, J.-M.; Habibi, Y.; Murariu, M.; Dubois, P. Polylactide (PLA)-based nanocomposites. *Prog. Polym. Sci.* **2013**, *38*, 1504–1542. [CrossRef]
2. Cardoso, L.; Usero, R.; Catani, S.M.M.; Barbo, M.L.P.; Esposito, A.R.; Duek, E.A.R. Implante de membranas de PLLA/Trietil-citrato como alternativa no tratamento de feridas cutâneas. *Polímeros Ciência Tecnol.* **2013**, *23*, 798–806. [CrossRef]
3. Meyers, M.A.; Chen, P.-Y.; Lin, A.Y.-M.; Seki, Y. Biological materials: Structure and mechanical properties. *Prog. Mater. Sci.* **2008**, *53*, 1–206. [CrossRef]
4. Nejati, E.; Mirzadeh, H.; Zandi, M. Synthesis and characterization of nano-hydroxyapatite rods/poly(l-lactide acid) composite scaffolds for bone tissue engineering. *Compos. Part A Appl. Sci. Manuf.* **2008**, *39*, 1589–1596. [CrossRef]
5. Armentano, I.; Dottori, M.; Fortunati, E.; Mattioli, S.; Kenny, J.M. Biodegradable polymer matrix nanocomposites for tissue engineering: A review. *Polym. Degrad. Stab.* **2010**, *95*, 2126–2146. [CrossRef]
6. Tirapelli, C.; Panzeri, H.; Soares, R.G.; Peitl, O.; Zanotto, E.D. A novel bioactive glass-ceramic for treating dentin hypersensitivity. *Braz. Oral Res.* **2010**, *24*, 381–387. [CrossRef] [PubMed]
7. Martins, C.H.G.; Carvalho, T.C.; Souza, M.G.M.; Ravagnani, C.; Peitl, O.; Zanotto, E.D.; Panzeri, H.; Casemiro, L.A. Assessment of antimicrobial effect of Biosilicate® against anaerobic, microaerophilic and facultative anaerobic microorganisms. *J. Mater. Sci. Mater. Med.* **2011**, *6*, 1439–1446. [CrossRef] [PubMed]
8. Granito, R.N.; Rennõ, A.C.; Ravagnani, C.; Bossini, P.S.; Mochiuti, D.; Jorgetti, V.; Driusso, P.; Peitl, O.; Zanotto, E.D.; Parizotto, N.A.; et al. In vivo biological performance of a novel highly bioactive glass-ceramic (Biosilicate®): A biomechanical and histomorphometric study in rat tibial defects. *J. Biomed. Mater. Res. Part B Appl. Biomater.* **2011**, *97*, 139–147. [CrossRef]
9. Crovace, M.C.; Souza, M.T.; Chinaglia, C.R.; Peitl, O.; Zanotto, E.D. Biosilicate®—A multipurpose, highly bioactive glass-ceramic. In vitro, in vivo and clinical trials. *J. Non. Cryst. Solids* **2016**, *432*, 90–110. [CrossRef]
10. Dziadek, M.; Stodolak-zych, E.; Cholewa-kowalska, K. Biodegradable ceramic-polymer composites for biomedical applications: A review. *Mater. Sci. Eng. C* **2017**, *71*, 1175–1191. [CrossRef] [PubMed]
11. Charles-Harris, M.; Koch, M.A.; Navarro, M.; Lacroix, D.; Engel, E.; Planell, J.A. A PLA/calcium phosphate degradable composite material for bone tissue engineering: An in vitro study. *J. Mater. Sci. Mater. Med.* **2008**, *19*, 1503–1513. [CrossRef] [PubMed]
12. Rezwan, K.; Chen, Q.Z.; Blaker, J.J.; Boccaccini, A.R. Biodegradable and bioactive porous polymer/inorganic composite scaffolds for bone tissue engineering. *Biomaterials* **2006**, *27*, 3413–3431. [CrossRef] [PubMed]
13. Blaker, J.J.; Gough, J.E.; Maquet, V.; Notingher, I.; Boccaccini, A.R. In vitro evaluation of novel bioactive composites based on Bioglass-filled polylactide foams for bone tissue engineering scaffolds. *J. Biomed. Mater. Res. A* **2003**, *67*, 1401–1411. [CrossRef]
14. Cunha, D.A.L.V.; Inforçatti Neto, P.; Micocci, K.C.; Bellani, C.F.; Selistre-de-Araujo, H.S.; Silveira, Z.C.; Branciforti, M.C. Fabrication and characterization of scaffolds of poly(ε -caprolactone)/Biosilicate® biocomposites prepared by generative manufacturing process. *Int. J. Biomater* **2019**. [CrossRef]
15. Oliveira, M.; Santos, E.; Araújo, A.; Fechine, G.J.M.; Machado, A.V.; Botelho, G. The role of shear and stabilizer on PLA degradation. *Polym. Test.* **2016**, *51*, 109–116. [CrossRef]
16. McNeill, I.C.; Leiper, H.A. Degradation studies of some polyesters and polycarbonates—2. Polylactide: Degradation under isothermal conditions, thermal degradation mechanism and photolysis of the polymer. *Polym. Degrad. Stab.* **1985**, *11*, 309–326. [CrossRef]
17. Blaker, J.J.; Bismarck, A.; Boccaccini, A.R.; Young, A.M.; Nazhat, S.N. Premature degradation of poly(α-hydroxyesters) during thermal processing of Bioglass®-containing composites. *Acta Biomater.* **2010**, *6*, 756–762. [CrossRef] [PubMed]
18. Fan, Y.; Nishida, H.; Hoshihara, S.; Shirai, Y.; Tokiwa, Y.; Endo, T. Pyrolysis kinetics of poly(l-lactide) with carboxyl and calcium salt end structures. *Polym. Degrad. Stab.* **2003**, *79*, 547–562. [CrossRef]
19. Fan, Y.; Nishida, H.; Shirai, Y.; Endo, T. Racemization on thermal degradation of poly(L-lactide) with calcium salt end structure. *Polym. Degrad. Stab.* **2003**, *80*, 503–511. [CrossRef]
20. Murariu, M.; Dubois, P. PLA composites: From production to properties. *Adv. Drug Deliv. Rev.* **2016**, *107*, 17–46. [CrossRef]

21. Kopinke, F.-D.; Remmler, M.; Mackenzie, K.; Milder, M.; Wachsen, O. Thermal decomposition of biodegradable polyesters -11. Poly(lactic acid). *Polym. Degrad. Stab.* **1996**, *43*, 329–342. [CrossRef]
22. Di Lorenzo, M.L.; Rubino, P.; Cocca, M. Isothermal and non-isothermal crystallization of poly(l -lactic acid)/poly(butylene terephthalate) blends. *J. Appl. Polym. Sci.* **2014**, *131*. [CrossRef]
23. Santos, L.G.; Costa, L.C.; Pessan, L.A. Development of biodegradable PLA/PBT nanoblends. *J. Appl. Polym. Sci.* **2018**, *135*, 45951. [CrossRef]
24. Pan, P.; Zhu, B.; Kai, W.; Dong, T.; Inoue, Y. Polymorphic transition in disordered poly(l-lactide) crystals induced by annealing at elevated temperatures. *Macromolecules* **2008**, *41*, 4296–4304. [CrossRef]
25. Androsch, R.; Iqbal, H.M.N.; Schick, C. Non isothermal crystal nucleation of poly (l-lactic acid). *Polymer* **2015**, *81*, 151–158. [CrossRef]